Relaxometry, Luminescence Measurements, Electrophoresis, and Animal Biodistribution of Lanthanide(III) Complexes of Some Polyaza Macrocyclic Acetates Containing Pyridine

Won D. Kim,[†] Garry E. Kiefer,[‡] Frédéric Maton,[§] Kenneth McMillan,[‡] Robert N. Muller,[§] and A. Dean Sherry*,[†]

Department of Chemistry, University of Texas at Dallas, Richardson, Texas 75083-0688, Designed Chemicals R & D, Dow Chemical Co., Freeport, Texas 77541, and Department of Organic Chemistry and NMR Laboratory, Medical Faculty, University of Mons-Hainault, B-7000 Mons, Belgium

Received July 19, 1994[⊗]

Four Gd^{3+} complexes [$Gd(BP2A)^+$, $Gd(PC2A)^+$, $Gd(PCTA)^0$, and $Gd(BPO4A)^-$] with polyazamacrocyclic ligands that contain a pyridine moiety were prepared and examined for possible use as MRI contrast enhancement agents. We estimated the number of inner sphere water molecules (q_{Gd}) for the Gd^{3+} complexes from the values of q found for the Tb^{3+} and/or Eu^{3+} complexes by luminescence lifetime measurements. We have estimated that q_{Gd} = 3.5, 3.3, 2.4, and 0.2 for $Gd(BP2A)^+$, $Gd(PC2A)^+$, $Gd(PCTA)^0$, and $Gd(BPO4A)^-$, respectively. The inner sphere relaxivities ($r_{1,inner}$) of these tetraaza macrocyclic complexes were higher than that of $Gd(DOTA)^-$ [i.e. 6.79 for $Gd(BP2A)^+$, 6.21 for $Gd(PC2A)^+$, and 4.60 for $Gd(PCTA)^0$ $mM^{-1}s^{-1}$ at 40 MHz and 25 °C], but the normalized relaxivities per q_{Gd} (1.94, 1.88, and 1.92 mM^{-1} s^{-1}, respectively) were comparable to that of $Gd(DOTA)^-$. A quantitative treatment of the NMRD profiles based on Solomon–Bloembergen–Morgan theory, using the NMRD profile of $Gd(BPO4A)^-$ to correct for an outer sphere contribution, showed that the complexes exhibit characteristics similar to that of $Gd(DOTA)^-$ but with shorter electronic relaxation times. Tissue biodistribution results using radioactive ^{153}Sm and ^{159}Gd complexes in rats indicate that the cationic [$^{153}Sm(BP2A)^+$ and $^{153}Sm(PC2A)^+$] complexes accumulate preferably in the bone tissue while the neutral [$^{153}Sm(PCTA)^0$] and anionic [$^{153}Sm(BPO4A)^-$] complexes appear to have renal clearances similar to those of other low molecular weight contrast agents [i.e. $Gd(DTPA)^{2-}$ and $Gd(DOTA)^-$].

Introduction

In recent years, polyaza macrocyclic paramagnetic metal ion chelates are finding many applications in biomedicine, especially as bioconjugates for monoclonal antibody radioisotope labeling[1] and as magnetic resonance imaging (MRI) agents. The tetraacetate analog DOTA, derived from tetraazacyclododecane, CYCLEN, forms one of the most stable (thermodynamically) and inert (kinetically) complexes with the trivalent lanthanide metal cations of any chelate evaluated to date.[2] These properties make $Gd(DOTA)^-$ one of the most effective and safest MRI contrast enhancement[3] agents available.[4] The complexes formed between lanthanide metals and the tetramethylenephosphonate analog, DOTP, have also been examined in some detail,[5] and the Tm^{3+} complex, $Tm(DOTP)^{5-}$, is proving to be a versatile $^{23}Na^+$ shift agent, both for perfused tissues and for *in vivo* animal studies.

Current interest in the complexation properties of macrocyclic ligands has led to the synthesis of many new macrocycles derived from cyclic polyaza and/or polyoxo ligands with a variety of ionizable pendent ligating groups.[6] We have continued to search for new macrocyclic derivatives which form stable lanthanide complexes with differing net charges and lipophilicities. As a part of our continuing effort, we report here on some chemical and magnetic properties of lanthanide complexes containing a pyridine moiety as part of their macrocyclic ring. The structures of these ligands, PC2A, PCTA, BP2A, and BPO4A, are shown below.

The synthesis and potentiometry of PC2A and BP2A and the X-ray crystal structure of $BP2A{\cdot}2HCl{\cdot}3H_2O$ are described in a companion paper.[7] The ligands PCTA and BPO4A are previously known. Stetter et al.[8] first reported the synthesis of PCTA and its complexation properties with alkaline earth (Mg^{2+}, Ca^{2+}, Sr^{2+}, and Ba^{2+}) and transition metal (Cu^{2+}, Pb^{2+}, Cd^{2+}, Co^{2+}, Zn^{2+}, Ni^{2+}, and Mn^{2+}) cations. The synthesis of BPO4A has been described in a patent[9] and some of its complexation characteristics were described in a recent abstract.[10]

* To whom correspondence should be addressed.
† University of Texas at Dallas.
‡ Dow Chemical Co.
§ University of Mons-Hainault.
⊗ Abstract published in *Advance ACS Abstracts,* March 15, 1995.

(1) (a) Moi, M. K.; Meares, C. F.; DeNardo, S. J. *J. Am. Chem. Soc.* **1988**, *110*, 6266. (b) Deshpande, S. V.; DeNardo, S. J.; Kukis, D. L. Moi, M. K.; McCall, M. J.; DeNardo, G. L.; Meares, C. F. *J. Nucl. Med.* **1990**, *31*, 473.
(2) (a) Cacheris, W. P.; Nickle, S. J.; Sherry, A. D. *Inorg. Chem.* **1987**, *26*, 958. (b) Brucher, E.; Laurenczy, G.; Makra, Z. *Inorg. Chim. Acta* **1987**, *139*, 141. (c) Wang, X; Jin, T.; Comblin V.; Lopez-Mut, A.; Merciny, E.; Desreux, J. F. *Inorg. Chem.* **1992**, *31*, 1095.
(3) Runge, V. M. *Enhanced Magnetic Resonance Imaging*; C. V. Mosby Co.: St. Louis, MO, 1989.
(4) (a) Geraldes C. F. G. C.; Sherry, A. D.; Brown, R. D., III; Koenig, S. H. *Magn. Reson. Med.* **1986**, *3*, 242. (b) Magerstaedt, M.; Gansow, O. A.; Brechbiel, M. W.; Colcher, D.; Baltzer, L.; Knop, R. H.; Girton, M. E.; Naegele, M. *Magn. Reson. Med.* **1986**, *3*, 808. (c) Muller, R. N.; Elst, L. V.; Rinck, P. A.; Vallet, R.; Masom, F.; Fischer, H.; Roch, A.; Haverbeke, Y. V. *Invest Radiol.* **1988**, *23*, 5229. (d) Sherry, A. D.; Brown, R. D., III; Geraldes, C. F. G. C.; Koenig, S. H.; Kuan, K. T.; Spiller, M. *Inorg. Chem.* **1989**, *28*, 620. (e) Bousquet, J. C.; Saini, S.; Stark, D. D.; Hahn, P. F.; Niigam, M.; Wittenberg, J.; Ferrucci, J. T. *Radiology* **1988**, *166*, 693. (f) Runge, V. M.; Gelblum, D. Y.; Paccetti, M. L.; Carolan, F.; Heard, G. *Radiology* **1990**, *177*, 393.
(5) (a) Lázár, I.; Hrncir, D. C.; Kim, W. D.; Kiefer, G. E.; Sherry, A. D. *Inorg. Chem.* **1992**, *31*, 4422. (b) Geraldes, C. F. G. C.; Sherry, A. D.; Kiefer, G. E. *J. Magn. Reson.* **1992**, *97*, 290. (c) Sherry, A. D.; Geraldes, C. F. G. C.; Cacheris, W. P. *Inorg. Chim. Acta.* **1987**, *139*, 137. (d) Sherry, A. D.; Malloy, C. R.; Jefferey, F. M. H.; Cacheris, W. P.; Geraldes, C. F. G. C. *J. Magn. Reson.* **1988**, *76*, 528.
(6) Izatt, R. M.; Pawlak, K.; Bradshaw, J. S. *Chem. Rev.* **1991**, *91*, 1721.
(7) Kim, W. D.; Hrncir, D. C.; Kiefer, G. E.; Sherry, A. D. *Inorg. Chem.* **1995**, *34*, 2225.
(8) Stetter, H.; Frank, W.; Mertens, R. *Tetrahedron* **1981**, *37*, 767.

0020-1669/95/1334-2233$09.00/0

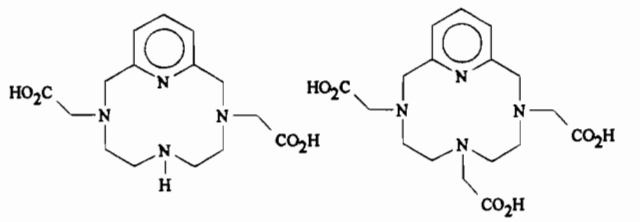

PC2A PCTA

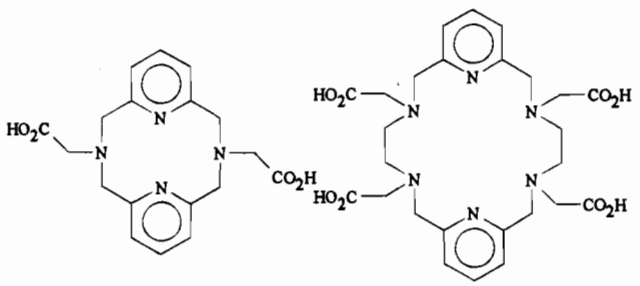

BP2A BPO4A

This report includes a determination of the number of inner sphere water molecules, q, by measuring the luminescence lifetimes of the Tb^{3+} and/or Eu^{3+} complexes, a determination of total net charge on the Tb^{3+} complexes at physiological pH by electrophoretic separation, a characterization of the magnetic properties of the Gd^{3+} complexes by recording nuclear magnetic relaxation dispersion profiles (NMRD) under various conditions, and animal tissue biodistribution results using radioactive ^{153}Sm or ^{159}Gd complexes.

Experimental Section

Ligands Synthesis. The synthesis and full characterization of PC2A and BP2A including the X-ray crystal structure of BP2A·2HCl·3H_2O have been described in a companion paper. The ligands PCTA[8] and BPO4A[9] are previously known and details of the preparation and X-ray crystal structure of PCTA·3Na·8H_2O and BPO4A·4HCl·4H_2O are reported elsewhere.[11] The preparation of the parent macrocyclic amines of PCTA and BPO4A (py[12]aneN_4 and py_2[18]aneN_6, respectively) were achieved using the classical Richman−Atkins method.[12] Previous literature preparations of py_2[18]aneN_6 have involved a template synthesis using either Ca(II)[9] or Ba(II).[13]

Complex Formation. The lanthanide complexes were formed in solution by mixing $LnCl_3$ (where Ln = Eu, Gd, Tb or Sm) with a 5% stoichiometric excess of each ligand. In a typical complex formation experiment, 1.00 mL of 0.1 M $LnCl_3$ solution was mixed with 1.05 mL of 0.1 M ligand, and the sample was neutralized with KOH and finally diluted to 5.00 mL to make a 20 mM stock solution of the complex. For storage and shipping of this stock solution, 1.00 mL of the stock solution was transferred into a vial, lyophilized, and sealed. The complex could be reconstituted later by simply adding appropriate amount of DI water to make a desired concentration (ca. add 4.00 mL of DI water to make 5 mM solution). All of the ligands form less stable complexes with Ln^{3+} cations than does DOTA, but they form complexes much faster than DOTA over the entire pH range.[7]

Luminescence Lifetimes. Luminescence lifetimes were measured with a Q-switched Continuum Model YG671C-10 Nd:YAG pulsed laser for excitation using a wavelength of 266 nm (fourth harmonic) and a pulse repetition rate of 10 Hz (~6 mJ/pulse), yielding a full width at half maximum, fwhm, of 5 ns. A CVI Digikrom 240 photomultiplier provided detection at either 544 nm (Tb·L) or 622 nm (Eu·L). Data were collected using a Tektronic DSA 602 digitizing signal analyzer and transferred to an AST Premium 386 PC (an IBM compatible PC) for analysis. Laser control and kinetic analyses were provided by the PC RAD and KS-01 software packages.[14] Ten to twenty repetitions, depending on signal intensities, were accumulated, averaged, and background noise (five repetitions, shutter closed) was subtracted. For determination of luminescence decay constants, both a single exponential decay fit and a floating baseline exponential decay fit were considered.

^{13}C NMR R_1 Measurements for the La(BP2A)$^+$ Complex. A ~40 mM solution of La(BP2A)$^+$ complex was prepared (including a small amount of D_2O for field locking) for ^{13}C T_1 measurements. All ^{13}C spectra were recorded on a General Electric GN-500 (11.7 T) spectrometer in a 5-mm tube while maintaining the temperature at 25 °C with a GE variable temperature accessory. A standard inversion recovery sequence ($\pi - t_D - \pi/2$−acquire, where t_D varied from 50 μs to 6 s) was used to record the data for the determination of the longitudinal relaxation rates, R_1 ($1/T_1$). The data were measured by ensuring that at a delay of at least $5T_1$ was allowed between successive pulse sequences to allow complete return of the spin system to equilibrium. The rate, R_1, was then evaluated by plotting $\ln(A_0 - A_t)$ vs t_D (50 μs , 1 ms, 50 ms, 0.1 s, 0.2 s, 0.5 s, 1 s, 2 s, 4 s, 6 s). The slope of the straight line plot is $-R_1$. The nuclear overhauser enhancement (NOE) factors, η, were determined using standard procedures.[15]

Electrophoresis. The electrophoretic mobilities of the Tb·L complexes were measured on cellulose paper (Whatman No. 3668-866) strips (2.5 × 20 cm) after exposure to a constant voltage (250 V) in 0.05 M HEPES buffer (Sigma) at pH = 7.4 for 1 h. The spots were visualized by placing the strips under a UV (254 nm) lamp.

NMRD Measurements. Proton relaxation dispersion profiles were measured using an IBM research field cycling relaxometer which measures the solvent water proton relaxation rate, R_1 ($1/T_1$), over a continuum of magnetic fields from 2 x 10^{-4} to 1.2 T (from 0.01 to 50 MHz proton Larmor frequency) under computer control with an absolute uncertainty in R_1 of 3%.[16] Additional single frequency measurements were performed on a Bruker MSL 200 (4.7 T) and on a Bruker PC20 (0.47 T) spin analyzer. Temperature regulation for the NMRD measurements was achieved by a thermostated circulating bath of perchloroethylene and was accurate to ±0.2 °C. The samples used in these experiments were prepared from lyophilized samples (20 μmol) by adding an appropriate amount of DI water (ca. 4.0 mL of DI water added to make 5 mM solution). Most NMR experiments were performed on a 1 mM solution with the pH stabilized around 7. To prepare more basic (ca. pH 12) samples, a small aliquot of NaOH was added to the 1 mM solution. R_1 was measured as function of complex concentration (0.1−5.0 mM), pH (7 and 12), and time (0 and 6 days) at 20 MHz and 39 °C. In addition, complete NMRD relaxivity profiles (0.01−40 MHz and at 200 MHz) were recorded at several temperatures (5, 15, 25, 37 °C).

Animal Biodistribution Studies. A stock $^{153}SmCl_3$ solution was prepared by adding 2 μL of 3 × 10^{-4} M $^{153}SmCl_3$ (radioactive) in 0.1 M HCl to 2 mL of a 3 × 10^{-4} M $SmCl_3$ carrier solution (on a few occasions, ^{159}Gd was used instead of ^{153}Sm). Appropriate ligand solutions were then prepared in DI water. After the two solutions were thoroughly mixed (pH ~ 2), the pH of the solution was raised to ~7 using 0.1 M NaOH to facilitate complexation. The completeness of complexation (for neutral and anionic complexes) was then evaluated by passing the sample solution (100 μL) through a Sephadex C-25 column eluting (2 × 3 mL) with 4:1 saline (0.85% NaCl/NH_4OH) and comparing the amount of radioactivity in the eluent vs on the column (free metal is retained on the column). For the cationic complexes, the technique described above was not applicable (since both the

(9) Carvalho, J. F.; Crofts, S. P.; Rocklage S. M. PCT Patent Application No. WO 91/10645 (EP 91/00126), July 25, 1991.
(10) Jackels, S. C.; Rothermel, G. L., Jr.; Bryant, L. H., Jr.; Miao, L.; Bell, D.; Fitzsimmons, P. M.; Lachgar, A. *Program and Abstracts*; XIX International Symposium on Macrocyclic Chemistry, Lawrence, Kansas; The University of Kansas: Lawrence, KS, 1994.
(11) Kim, W. D. D.Chem. Dissertation, The University of Texas at Dallas, Richardson, TX, 1994.
(12) Richman, J. E.; Atkins, T. J. *J. Am. Chem. Soc.* **1974**, *96*, 2268.
(13) Rothermel, G. L. Jr.; Miao L; Hill, A. L.; Jackels, S. C. *Inorg. Chem.* **1992**, *31*, 4854.
(14) Kinetic Instruments, P.O. Box 49434, Austin, TX 78765.
(15) Martin, M. L.; Delpuech, J. J.; Martin, G. L. *Practical NMR Spectroscopy*; Heyden and Sons: London, 1980.
(16) Koenig, S. H.; Brown, R. D., III *Prog. NMR. Spectrosc.* **1991**, *22*, 487.

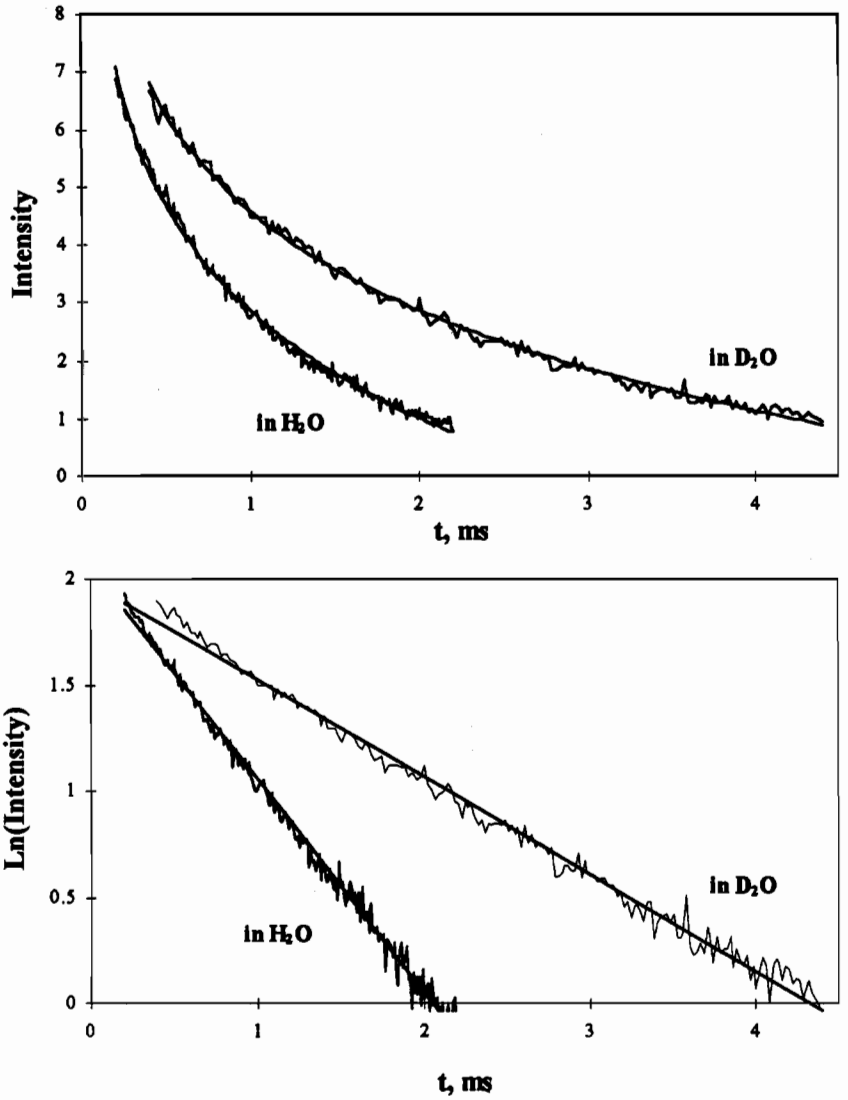

Figure 1. Luminescence decay curves in H_2O and D_2O for $Tb(BP2A)^+$ are shown in the upper plot. The bottom plots show ln(intensity) vs time for determination of the decay rate constants. The excitation wavelength was 266 nm, and the detection wavelength was 544 nm.

complex and the free metal are cationic). Thus complexation was achieved by stirring excess (5−10%) ligand with metal for 12 h and assuming complete complexation. The *in vivo* distribution of the radioactive complexes was measured using three to five Sprague−Dawley rats (180−220 g), each injected with 100 μL (pH = 7.5) of the radioactive complex solution. After either 30 min or 2 h, the animals were anesthetized and sacrificed. The following organs were dissected, weighed, and counted: bone, liver, kidney, spleen, muscle, and blood. The total percentage of the dose in bone was calculated by assuming that the bone sample (femur) represents $^1/_{25}$ the weight of the total skeleton and that the distribution of radioactivity was the same in femur and other bones. The total percentage of the dose in blood was calculated by assuming that blood comprised 6.5% of total body weight. The total percentage of the dose in muscle was calculated by assuming that muscle comprised 43% of total body weight.[17]

Absorption of Tb Complexes on Hydroxyapatite. A column (0.5 × 1.5 cm) containing hydroxyapatite (Sigma, Type I) was eluted with DI water (5 mL) prior to loading with a Tb complex (0.05 mL of 0.1 M solution). The column was further eluted with DI water (5 mL) and finally completely drained. The column material was then emptied and spread evenly on cellulose filter paper. The luminescence intensity of the column bed from each Tb complex was qualitatively compared after being placed under a UV (254 nm) lamp.

Results and Discussion

Luminescence Studies of the Tb^{3+} and Eu^{3+} Complexes. Studying the luminescence properties of the Gd^{3+} complexes directly is difficult due to their unfavorable molar absorptivity and weak luminescence in solution.[18] Thus, the Tb^{3+} and Eu^{3+} complexes were prepared for these studies. Since Tb and Eu are neighbors in the periodic table, we assumed that the Tb^{3+} [or Eu^{3+}] complexes are, in general, isostructural with the corresponding Gd^{3+} species. UV (266 nm) excitation of Tb^{3+} [Eu^{3+}] complexes results in very efficient generation of the luminescent excited state, via absorption by the pyridine moieties and transfer of the energy to the Tb^{3+} $^5D_4$ [Eu^{3+} $^5D_0$] excited state. In subsequent emissive transitions to the $^7F_6$, $^7F_5$, $^7F_4$, and $^7F_3$ [$^7F_4$, $^7F_3$, $^7F_2$, $^7F_1$, and $^7F_0$] states, the complexes luminesce strongly (fluorescence was easily visualized). Among the emission peaks, the $^7F_5$ (544 nm) [$^7F_2$ (622 nm)] peak is the most intense and the results obtained in this study are from an analysis of $^5D_4 \rightarrow {}^7F_5$ [$^5D_0 \rightarrow {}^7F_2$] transition.

The number of inner sphere water molecules in the Tb^{3+} [Eu^{3+}] complexes in an aqueous solution was determined by measuring the luminescence lifetimes of complexes in H_2O and

(17) Goeckeler, W. F.; Edwards, B.; Wolkert, W. A.; Holmes, R. A.; Simon, J.; Wilson, D. *J. Nucl. Med.* **1987**, *28*, 495.

(18) Chang, C. A.; Brittain, H. G.; Telser, J.; Tweedle, M. F. *Inorg. Chem.* **1990**, *29*, 4468.

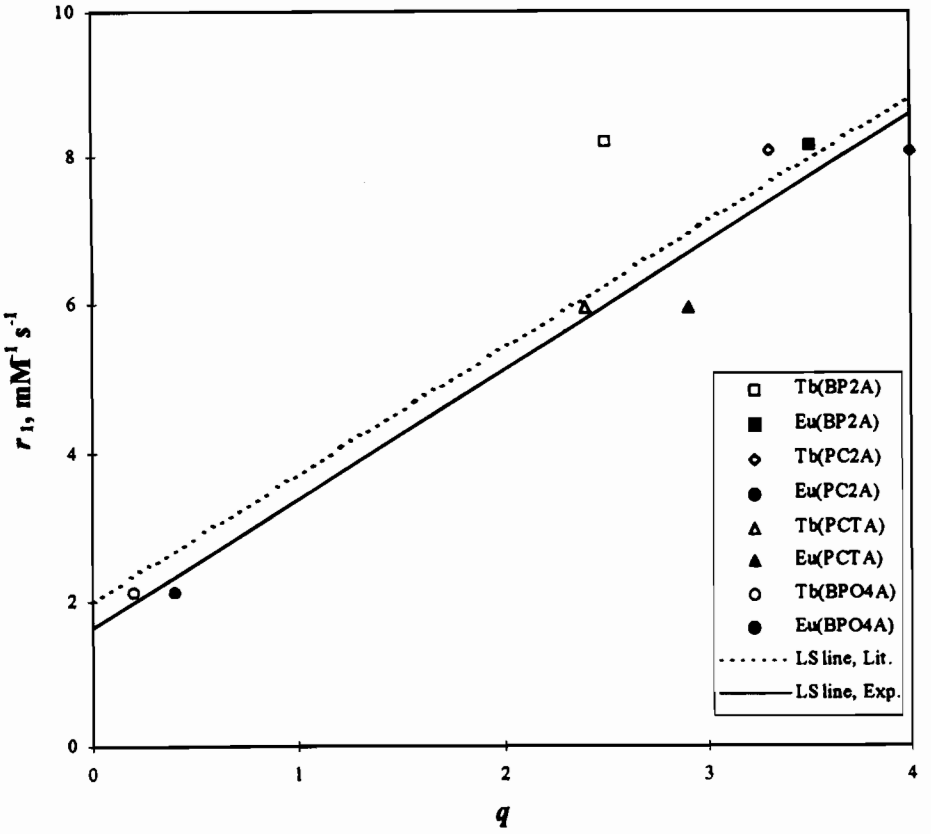

Figure 2. Plot of relaxivities, r_1, determined at 20 MHz and 39 °C vs number of inner sphere water molecule, q, determined from the luminescence lifetime measurements. The solid line is the linear least-squares line of the data from this study and the broken line was adopted from the literature,[21] 20 MHz and 40 °C.

Table 1. Number of Inner Sphere Water, q, Determined

	k_H, ms^{-1}	k_D, ms^{-1}	q
$Tb(PC2A)^+$	1.56	0.77	3.3
$Tb(BP2A)^+$	1.06	0.47	2.5
Tb(PCTA)	1.28	0.72	2.4
$Tb(BPO4A)^-$	0.29	0.25	0.2
$Eu(PC2A)^+$	8.05	4.21	4.0
$Eu(BP2A)^+$	4.23	0.82	3.5
Eu(PCTA)	3.69	0.95	2.9
$Eu(BPO4A)^-$	2.86	2.52	0.4

D_2O.[19] Deactivation of the $^5D_4$ [$^5D_0$] excited state of Tb^{3+} [Eu^{3+}] is strongly enhanced by coupling with the O-H stretching modes of coordinated water molecules. Therefore, the excited state lifetime of Tb^{3+} [Eu^{3+}] is shorter in H_2O than in D_2O. The number of coordinated water molecules, q, is related to the excited state lifetimes as shown in eq 1, where, k_H and k_D

$$q = m(k_H - k_D) \quad (1)$$

are the luminescence decay rate constants (ms^{-1}, the reciprocals of the lifetime) of Tb^{3+} [Eu^{3+}] complexes in H_2O and D_2O, respectively. The proportionality constant m (4.20 ms for Tb^{3+} and 1.05 ms for Eu^{3+}) is the value previously reported[19] from luminescence and crystallographic studies of various Tb^{3+} and Eu^{3+} complexes.

Examples of the luminescence decay curves for $Tb(BP2A)^+$ are shown in Figure 1 as an illustration. The rate constants (k_H and k_D), and values of q are summarized in Table 1. The data indicate that the value of q for $Tb(BP2A)^+$ and $Eu(BP2A)^+$ complexes are significantly different even after accounting for an estimated uncertainty of about 0.5 with this technique.[19] This discrepancy must reflect a discontinuous change in q across the lanthanide series.[20] To decide which q value is correct for $Gd(BP2A)^+$, we plotted r_1 (20 MHz, 39 °C) values for each of the Gd^{3+} complexes examined in this study vs q values obtained from the corresponding Tb^{3+} and Eu^{3+} complex luminescence lifetimes (Figure 2). Also shown is the linear regression (dotted line) reported previously for a series of other Gd^{3+} complexes.[21] This plot indicates that r_1 for the Gd^{3+} complexes correlates well with the q values of the corresponding Tb^{3+} and Eu^{3+} complexes, except for $Tb(BP2A)^+$. The value of q measured for the $Eu(BP2A)^+$ complex however fits the relationship quite well. A linear least squares analysis of r_1 vs q, excluding the $Tb(BP2A)^+$ point, gives a correlation coefficient (R^2) of 0.9638 with an intercept of 1.6 ± 0.4 ($mM^{-1} s^{-1}$), and a slope of 1.7 ± 0.2 ($mM^{-1} s^{-1}$). These parameters are in good agreement with the values reported in the literature[21] for a series of simple mononuclear and highly hydrophilic Gd^{3+} amino carboxylate complexes. This relationship was the basis of our conclusion that $Gd(BP2A)^+$ and $Eu(BP2A)^+$ are isostructural [but not $Tb(BP2A)^+$], while the Gd^{3+} and Tb^{3+} complexes of the remaining analogues are isostructural. The q_{Gd} (estimated q in Gd^{3+} complex) determined here was used later in an evaluation of the distance of closest approach of water protons from the metal center, r, in a quantitative treatment of the NMRD data.

Determination of τ_R of $Gd(BP2A)^+$. The rotational correlation time (τ_R) of $La(BP2A)^+$ was estimated by measuring ^{13}C spin-lattice relaxation rates (R_1) and NOE factors, η, for all carbon atoms in the complex. The τ_R for the three types of

(19) Horrocks, W. D.; Sudnick, D. R. *J. Am. Chem. Soc.* **1979**, *101*, 334.

(20) (a) Spedding, F. H.; DeKoch, C. W.; Pepple, G. W.; Habenschuss, A. *J. Chem. Eng. Data* **1977**, *22*, 58. (b) Choppin, G. R. *Pure Appl. Chem.* **1971**, *27*, 23.

(21) Zhang, X.; Chang, C. A.; Brittain, H. G.; Garrison, J. M.; Telser, J.; Tweedle, M. F. *Inorg. Chem.* **1992**, *31*, 5597.

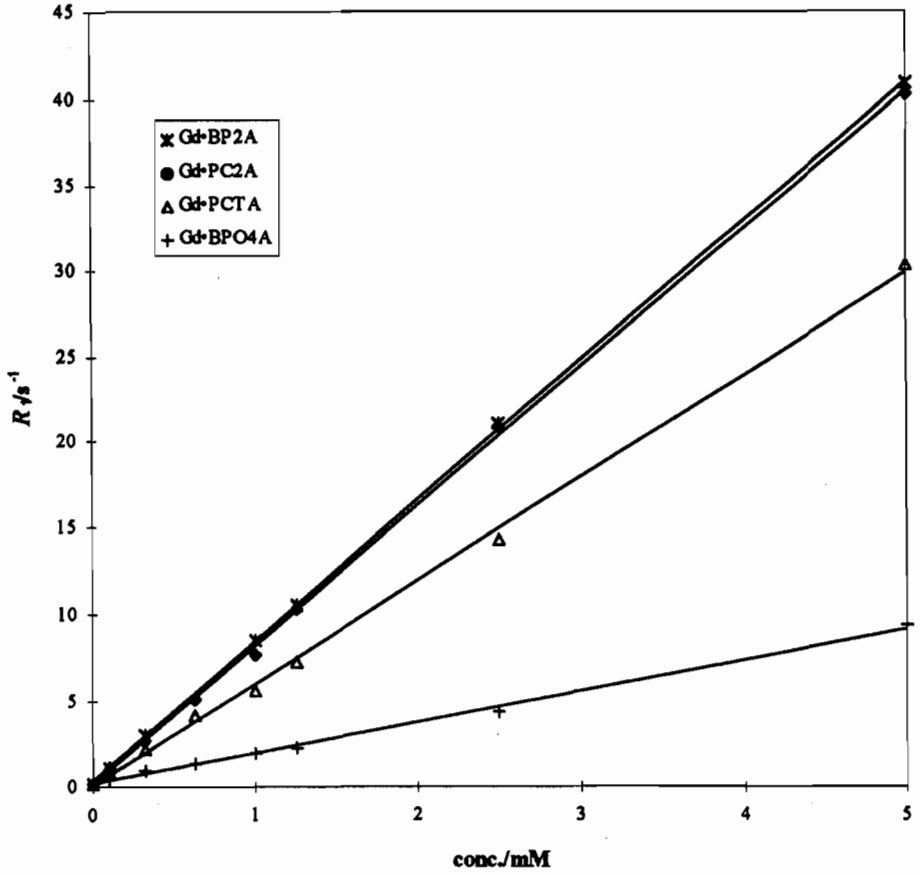

Figure 3. Plot of relaxation rate, R_1, vs complex concentrations (0.1−5.0 mM). Plots show that the relationships are perfectly linear indicating that microviscosity effect or agglomeration is not a factor influencing τ_R.

Table 2. Rotational Correlation Time, τ_R, of La(BP2A)$^+$ Determined at 25 °C from ^{13}C-NMR R_1 and η

carbon	N	R_1, s^{-1}	η	R_1^{DD}, s^{-1}	τ_R, ps
4-py	1	4.33	0.56	1.22	54
3,5-py	1	3.65	0.79	1.45	64
py-$CH_{2\text{-}N}$	2	5.33	1.20	3.22	71

carbons (4-py, 3,5-py, and py-CH_2-N) were determined independently. The dipolar contribution (R_1^{DD}) to R_1 for each carbon may be determined from the experimental η values (eq 2), where

$$R_1^{DD} = \frac{\eta}{\eta_{max}} R_1 \qquad (2)$$

η_{max} is the maximum possible NOE (ca. 1.988). Given R_1^{DD}, the correlation time can be estimated using eq 3,[22] where, r_{CH}

$$\tau_R = \frac{R_1^{DD} r_{CH}^6}{N\left(\frac{\mu_0}{4\pi}\right)\gamma_C^2\gamma_H^2\hbar^2} \qquad (3)$$

is the C−H bond length (ca. 1.08 Å), N is the number of directly bonded protons on each carbon, and the other parameters have their usual meanings (physical constants). The results of such calculations are summarized in Table 2. Given the assumption that the size of La(BP2A)$^+$ and Gd(BP2A)$^+$ and their mobilities in solution are similar, these results were used to evaluate the distance of closest approach of water protons to the Gd^{3+} center, **r** (see below).

(22) Neuhause, D.; Williamson. M. *The Neuclear Overhauser Effect in Structural and Conformational Analysis*; VCH Publishers, Inc.: New York, 1989.

NMRD Studies. In NMRD, the spin−lattice relaxation time ($1/T_1$) of the bulk water protons is measured as function of magnetic field strength in the presence of a solute that facilitates relaxation. The solute that facilitates water relaxation is, in this case, the paramagnetic metal ion that is complexed with an organic ligand. A variety of mechanisms are responsible for the relaxation of bulk water protons. The dominant mechanisms of relaxation can be deduced from the NMRD profile, thereby determining how water molecules interact with the paramagnetic metal center in the complex.

The water proton relaxation rate (20 MHz, 39 °C) was found to be linear with complex concentration over the range 0.1−5 mM (Figure 3). If the relaxation rates are governed by τ_R at this frequency, then the observed linearity indicates that no significant aggregation of these complexes occurs over this concentration range.

A higher water relaxivity has been reported for Mn(DPDP) at pH 11 than at pH 7.[23] This enhancement at high pH was thought to be due to the two pyridine groups in this ligand (see structure below), which might either alter the closest approach

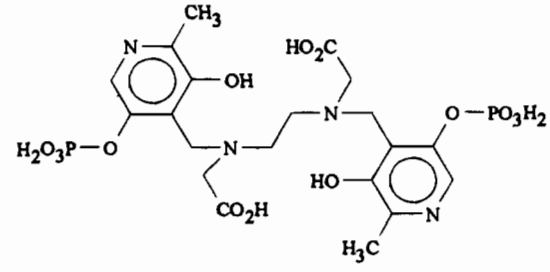

DPDP

Table 3. Time and pH Dependent r_1 and r_2 at 20 MHz, 39 °C

	Time: 0 day				Time: 6 days	
	pH=7		pH = 12		pH = 7	pH = 12
	r_1	r_2	r_1	r_2	r_1	r_1
$Gd(PC2A)^+$	7.50 ± 0.20	8.30 ± 0.70	3.70 ± 0.03	3.90 ± 0.15	7.57 ± 0.20	3.60 ± 0.05
Gd(PCTA)	5.42 ± 0.12	6.52 ± 0.28	3.43 ± 0.12	3.11 ± 0.09	5.70 ± 0.11	4.54 ± 0.09
$Gd(BP2A)^+$	8.27 ± 0.34	8.63 ± 0.37	4.51 ± 0.07	4.91 ± 0.11	8.02 ± 0.08	3.98 ± 0.02
$Gd(BPO4A)^-$	1.71 ± 0.09	1.74 ± 0.09	1.66 ± 0.11	1.83 ± 0.19	1.67 ± 0.03	1.55 ± 0.23

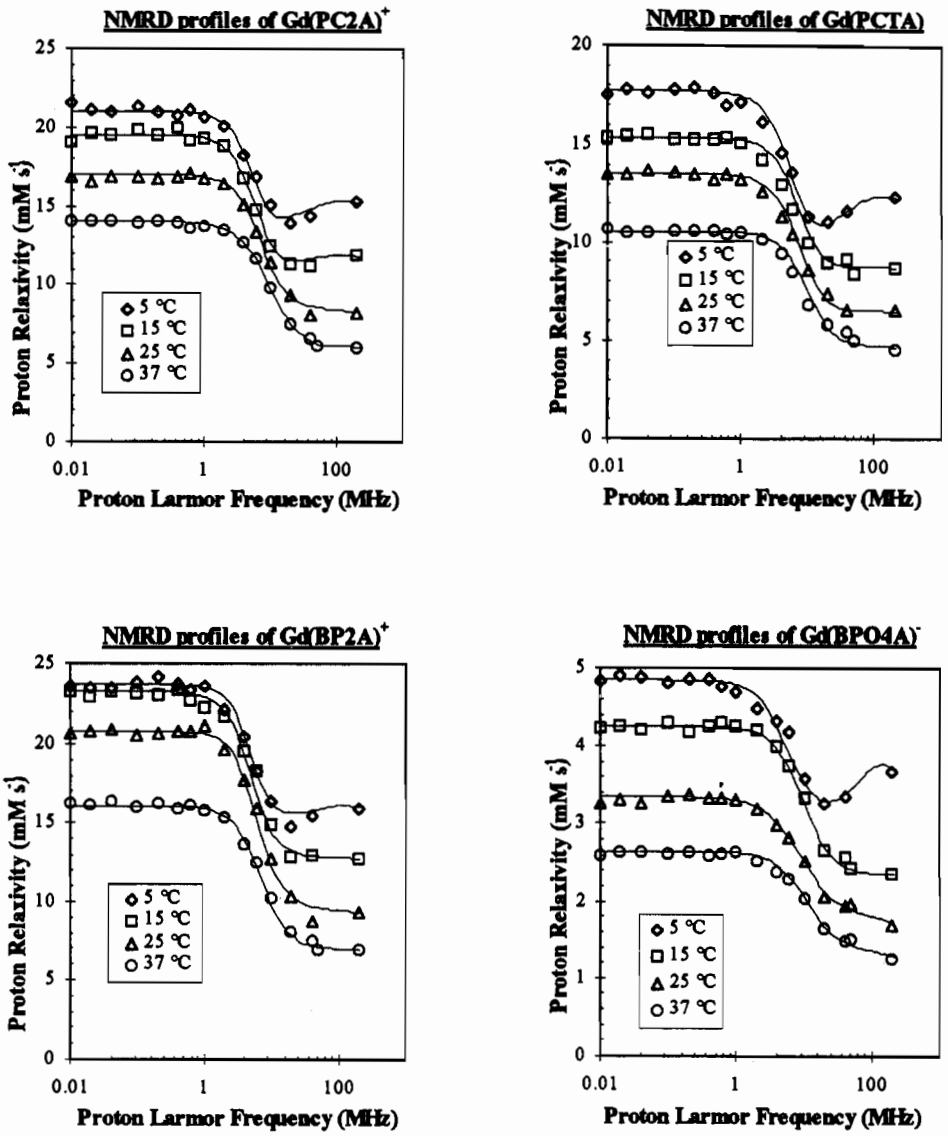

Figure 4. NMRD curves of complexes examined in this study at several temperatures. The lines through the data points were calculated using Solomon–Bloembergen–Morgan theory with the parameters outlined in the text.

of water molecules into the metal center, or enhance the relaxation by delocalizing electron spin onto the pyridine moieties. None of the new complexes we have studied here have parallel behavior. In all cases, the relaxivity is lower at pH 12 than at pH 7 (see Table 3).

This decrease in relaxivity at high pH can arise from a reduction of the hydration number in the basic medium by the partial substitution of water molecules by OH^- ligands or by partial precipitation (although not visibly obvious). Note that the relaxivity of $Gd(BPO4A)^-$ is not pH dependent and this complex is the only one in this family of complexes that does not have an inner sphere water molecule (see Table 1). A small degree of complex instability (where $q > 0$) was observed in the pH range from 7 to 12 as evidenced by gradual decreases in r_1 over 6 days. However at pH 7 the complexes showed no sign of degradation. The relaxivities measured at pH 7 do not change during this period and we thus conclude that the complexes are stable in neutral solution.

Figure 4 shows the temperature dependent NMRD relaxivity profiles of $Gd(PC2A)^+$, Gd(PCTA), $Gd(BP2A)^+$, and $Gd(BPO4A)^-$, respectively. The lines through the data points were calculated using Solomon–Bloembergen–Morgan (SBM) theory[24] with the parameters determined in this study. A

(23) Maton, F. Ph.D. Thesis, University of Mons-Hainault, Mons, Belgium, 1993.

(24) (a) Aime, S.; Botta, M.; Ermond, G.; Fedeli, F.; Uggeri, F. *Inorg. Chem.* **1992**, *31*, 1100. (b) Tweedle, M. F. *J. Alloys Compd.* **1992**, *180*, 317.

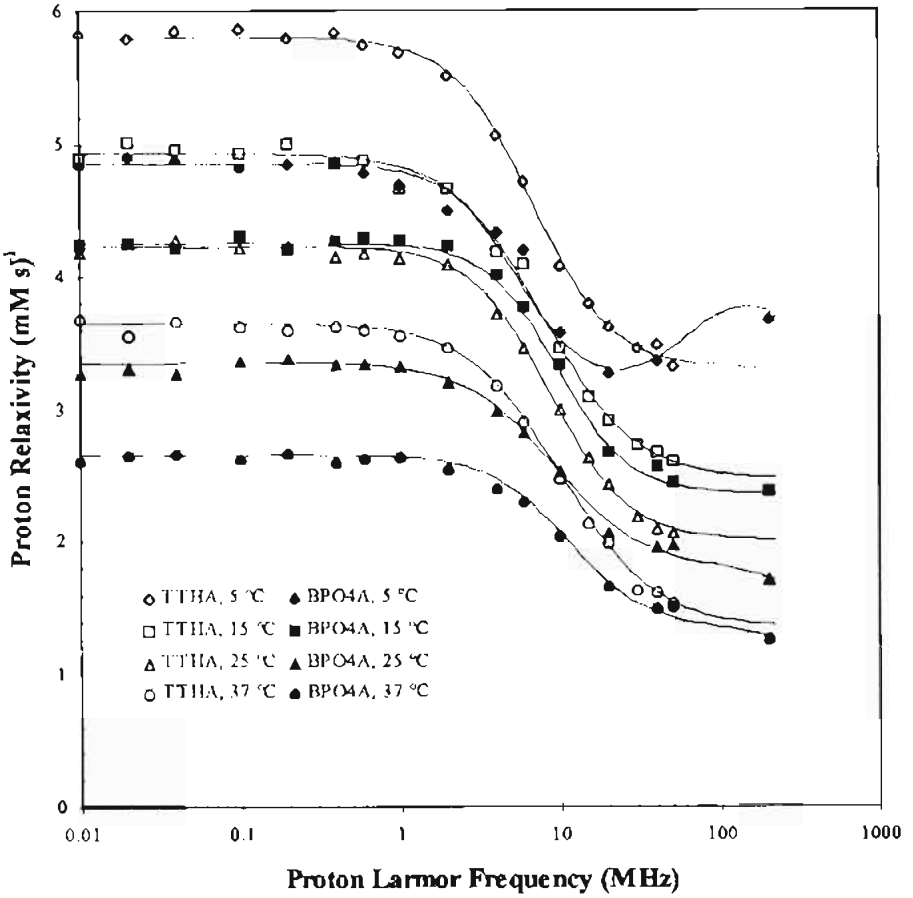

Figure 5. NMRD profiles of $Gd(BPO4A)^-$ compared with $Gd(TTHA)^{3-}$ profiles at several temperatures.

quantitative treatment of these NMRD data based on standard inner sphere relaxation theory requires the subtraction of an outer sphere contribution (OS) from the observed relaxivity of the complexes. We have chosen the relaxivity of the Gd(BPO4A) as the OS contribution, since its hydration number (q) was shown to be no greater than 0.2 (from luminescence experiments). This compound exhibits behavior similar to that of $Gd(TTHA)^{3-}$ which is known to have no ($q = 0$) water molecules in its first coordination sphere. Comparison of their NMRD profiles (Figure 5) shows that, over the temperature range 5−37 °C, the relaxivity of $Gd(BPO4A)^-$ differs from $Gd(TTHA)^{3-}$ only at low field where the relaxivity is mainly governed by electron spin relaxation (τ_{S0}).

The first step in fitting the NMRD profiles to the standard SBM model is to determine whether τ_M, the lifetime of the water molecule in the coordination sphere of Gd^{3+}, contributes to r_1. For this purpose, we compare the temperature dependence of the r_1 value of the new complexes to the r_1 values of $Gd(DOTA)^-$ at 0.01 MHz and 40 MHz. It has been reported[25] that the residence lifetime of a water molecule in the first coordination sphere of $Gd(DOTA)^-$ does not influence the relaxation process. In order to compare the relaxivities of complexes with different q, we normalized the inner sphere relaxivity to the contribution provided by one water molecule ($q = 1$) (Figure 6). At high field (40 MHz), the new complexes behave like $Gd(DOTA)^-$. It is thus likely that the $r_{1,inner}$ of these complexes is governed by τ_R since $Gd(DOTA)^-$ is characterized by a "silent" τ_M. At low field, however, the $r_{1,inner}$ values of the complexes in this study were lower than that of $Gd(DOTA)^-$, indicating that the pyridine based systems have a shorter electronic relaxation time (τ_{S0}). This means that compared to $Gd(DOTA)^-$, the $r_{1,inner}$ values of the pyridine-based complexes are not limited by τ_M ($\tau_M < T_{1M,low\ field}$). Since the normalized high field relaxivities of the pyridine-based complexes are similar to those of Gd(DOTA)$^-$, one would expect that the ratio, τ_R/r^6, at high fields to be identical for the whole series of compounds (eq 4). Since the molecular sizes are similar, as evidenced by a τ_R for $La(BP2A)^+$ of 64 ps (average in Table 2) vs a τ_R of 50−70 ps[24] for low molecular complexes such as $Gd(DOTA)^-$ or $Gd(DTPA)^{2-}$, the distance of the closest approach of water molecules in the pyridine-based complexes will also not differ much from that found in Gd(DOTA)$^-$.

This was verified by experiments performed at 4.7 T (200 MHz). At this field, the high field inner sphere relaxivity may be approximated by the well-known equation

$$r_{1,inner} \equiv \varrho q B \frac{\tau_R}{r^6} \tag{4}$$

where, ϱ is the mole fraction of paramagnetic complex, q is the number of water molecules bound per metal ion, B represents combined constants including γ_I (proton gyromagnetic ratio), g (electronic g-factor), S (total electron spin of the metal ion), and β (Bohr magneton), and r is the proton−metal ion distance. This relationship was applied to calculate the closest approach of water protons to $Gd(BP2A)^+$ from the relaxivity measured at 200 MHz and 25 °C. The value of q was estimated from the luminescence lifetime data and τ_R from the relaxation rates of the $La(BP2A)^+$ complex, substituting the following constants

$$\langle r \rangle = \left[\varrho \langle q \rangle B \frac{\langle \tau_R \rangle}{\langle r_{1,inner} \rangle} \right]^{1/6} \tag{5}$$

(25) Micskei, K.; Helm, L.; Brücher, E.; Merbach, A. E. *Inorg. Chem.* **1993**, *32*, 3844.

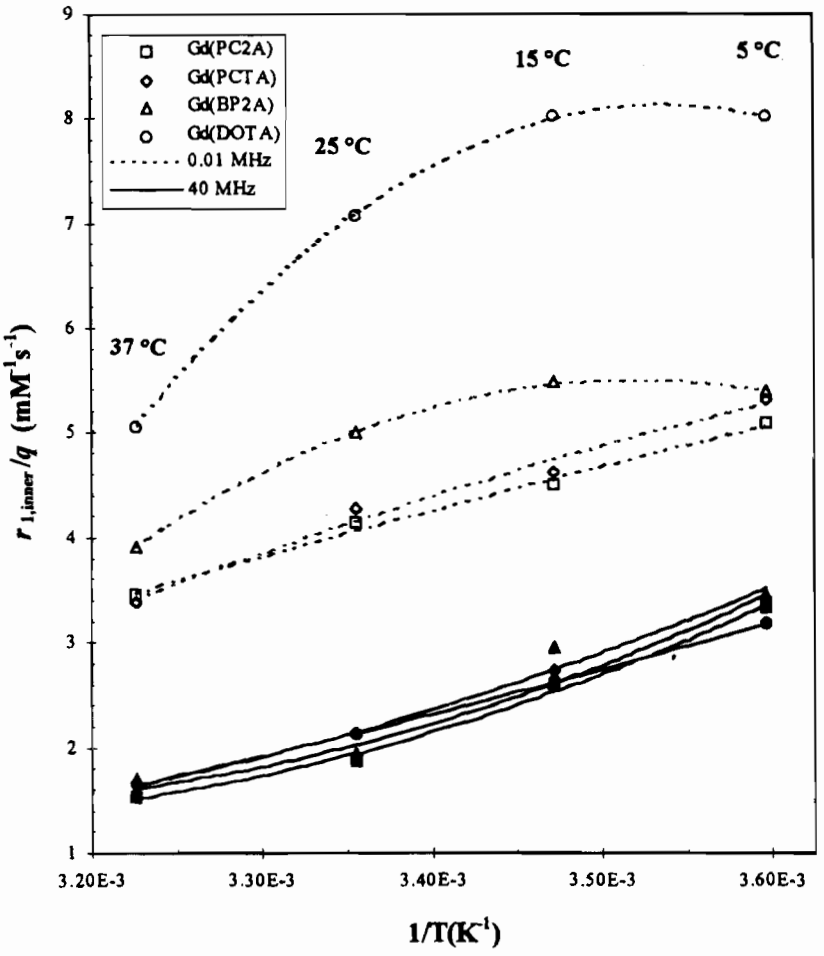

Figure 6. Temperature (5−37 °C) dependence of inner sphere relaxivity per each water molecule bonded to the metal. Data are presented with $Gd(DOTA)^-$ values for comparison. For outer sphere corrections we used values from $Gd(BPO4A)^-$ for the pyridine containing complexes and $Gd(TTHA)^{3-}$ for $Gd(DOTA)^-$. Broken lines connect 0.01 MHz data and continuous lines connect 40 MHz data.

into eq 5 ($\varrho B = 2.788 \times 10^{-35}$ cm^6 s^{-2}, $\langle q \rangle = 3.5 \pm 0.35$, $\langle \tau_R \rangle = (6.4 \pm 0.8) \times 10^{-11}$ s, and $\langle r_{1,inner} \rangle = (7.60 \pm 0.07)$ mM^{-1} s^{-1}) yields $\langle \mathbf{r} \rangle = (3.06 \pm 0.12)$ Å.

This value was identical to the average distance observed for other Gd^{3+} complexes (3.13 Å).[26] This indicates that water relaxation in this pyridine-containing macrocyclic complex behaves as any other inner sphere complex and that there is no additional water relaxation due to delocalization of unpaired spin density onto the pyridine moiety.

Since the other complexes are similar (Figure 7), we used this $\langle \mathbf{r} \rangle$ value to fit the NMRD profiles of all compounds, taking in account their respective q values and neglecting τ_M (10 ns). The calculated relaxation parameters are summarized in Table 4. The error presented in the table reflects the quality of the fittings not the uncertainty in **r**. From the temperature dependence of τ_R, we calculated rotational activation parameters for each complex and found them to be similar to literature[25] values for $Gd(DTPA)^{2-}$ and $Gd(DOTA)^-$ (Table 5).

In summary, the new Gd(PC2A, PCTA, BP2A) complexes exhibit normal relaxivities taking into account their respective hydration numbers. They have relaxation characteristics comparable to $Gd(DOTA)^-$ but with shorter electronic relaxation times. The inner sphere relaxivities of the Gd^{3+} complexes examined here were governed primarily by their q values; we found no evidence of a relaxivity contribution from unpaired electrons delocalized into the pyridine rings.

(26) Lauffer, R. B. *Chem. Rev.* **1987**, *87*, 901.

Electrophoresis of Tb^{3+} Complexes. To confirm the charges on $Tb(PC2A)^+$, $Tb(PCTA)^0$, $Tb(BP2A)^+$, and $Tb(BPO4A)^-$, we performed paper electrophoretic separation of the aforementioned complexes in 0.05 M HEPES buffer at biological pH (7.4) for 1 h: $Tb(PC2A)^+$; 1.0 cm toward anode, $Tb(BP2A)^+$; 1.3 cm toward anode, $Tb(PCTA)^0$; no movement, $Tb(BPO4A)^-$; 1.0 cm toward cathode. The charge of complexes can be estimated by subtracting the number of acetate groups (charge on the organic ligand) from the charge of Tb(III) metal (i.e. for $Tb(BP2A)^+$, $3 - 2 = 1$). And, for all complexes we have studied, the expected net charges of each complexes was confirmed, Table 6.

In this experiment, the spots were easily located by shining UV light (short wavelength, 254 nm) onto the paper strip, even while the strips were developing. One could also determine that the complexes remained intact after being subjected to an electric field. If the complexes had fallen apart when subjected to this high electric field (250 V for 1 h) the luminescence would have disappeared because luminescence of free Tb(III) cannot be visualized under UV light.

Animal Biodistribution. The results of 2 hr animal biodistribution studies of $^{153}Sm(PC2A)^+$, $^{153}Sm(BP2A)^+$, $^{153}Sm(PCTA)^0$, and $^{153}Sm(BPO4A)^-$ are summarized in Figure 8 (Top) along with data for $^{153}Sm(DTPA)^{2-}$ and $^{153}Sm(DO2A)^+$,[7] for comparative purposes. The 30 min animal biodistributions for $^{153}Sm(PCTA)^0$, and $^{153}Sm(BPO4A)^-$ are compared in Figure 8 (bottom) with $^{153}Sm(DTPA)^{2-}$ data. Similar animal biodistributions were also obtained for some of the $^{159}Gd^{3+}$ complexes. The effect of variation in net charge of the complexes was

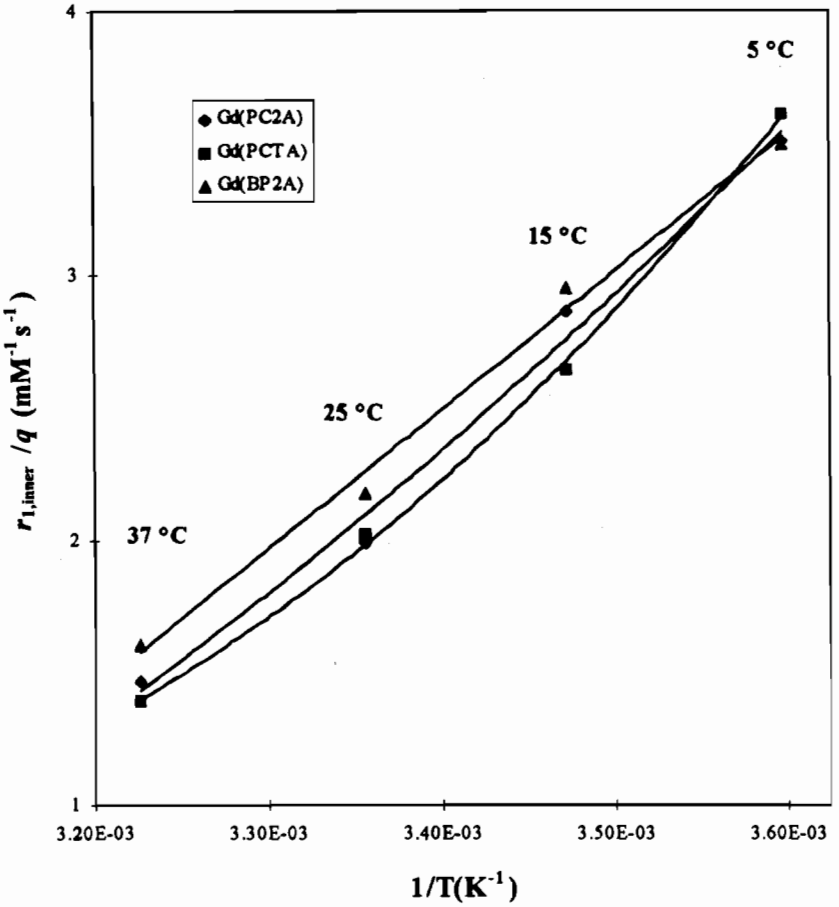

Figure 7. Temperature dependence of inner sphere relaxivity per each water molecule bonded to the metal at 200 MHz. Inner sphere contributions were determined by subtracting an outer sphere contribution [Gd(BPO4A)$^-$] from the experimentally observed relaxivities.

Table 4. Relaxation Parameters Determined at Various Temperatures

	τ_V, ps	τ_R, ps	τ_{S0}, ps
		Gd(PC2A)$^+$	
37	23 ± 3	40 ± 1	96 ± 3
25	27 ± 3	54 ± 1	93 ± 3
15	14 ± 1	79 ± 1	75 ± 2
5	27 ± 1	96 ± 1	71 ± 1
		Gd(PCTA)	
37	15 ± 2	44 ± 1	87 ± 3
25	21 ± 6	60 ± 4	104 ± 8
15	19 ± 1	80 ± 1	85 ± 2
5	24 ± 2	106 ± 2	87 ± 2
		Gd(BP2A)$^+$	
37	19 ± 1	47 ± 1	119 ± 5
25	42 ± 3	64 ± 1	140 ± 6
15	37 ± 3	87 ± 1	104 ± 2
5	35 ± 2	102 ± 1	89 ± 2

[a] τ_R: rotational correlation time. τ_{S0}: T_{1e} at zero field. τ_V: correlation time modulating electron spin relaxation. T_{1e}: longitudinal electron spin relaxation time.

Table 5. Rotational Activation Energies

complex	E_R, kJ mol^{-1}
Gd(PC2A)$^+$	19 ± 2
Gd(PCTA)	19.0 ± 0.3
Gd(BP2A)$^+$	16 ± 2
Gd(DOTA)$^-$	17 ± 3[a]
Gd(DTPA)$^{2-}$	18 ± 2[a]

[a] Misckei et al.[25]

clearly evident among the cationic and non-cationic complexes. The noncationic complexes [^{153}Sm(PCTA)^0, and ^{153}Sm(BPO4A)$^-$]

Table 6. Confirmation of Charges of Tb(III) Complexes by Electrophoresis

complex	charge on Tb	no. of Acetate Groups	charge of complex	mobility	remark	confirmed?
Tb(PC2A)$^+$	3	2	1	anode	cation	yes
Tb(PCTA)	3	3	0	none	neutral	yes
Tb(BP2A)$^+$	3	2	1	anode	cation	yes
Tb(BPO4A)$^-$	3	4	−1	cathode	anion	yes

were cleared from the body through the kidneys (see 30 min data in Figure 8) similar to other blood pool agents such as ^{153}Sm(DTPA)$^{2-}$. However, the cationic complexes ^{153}Sm(PC2A)$^+$, ^{153}Sm(BP2A)$^+$, and ^{153}Sm(DO2A)$^+$ showed unusually high bone uptake. Even after 2 h, 28%, 32%, and 42%, of the injected dose of ^{153}Sm(PC2A)$^+$,^{153}Sm(BP2A)$^+$, and ^{153}Sm(DO2A)$^+$, respectively, was localized in bone tissue.

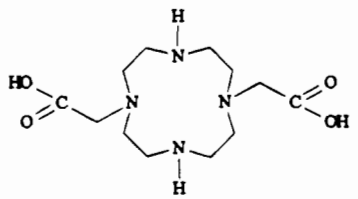

DO2A

It is well known that phosphonate-containing complexes are very effectively retained by bone and calcified tissues and are routinely used in nuclear medicine as bone imaging agents.[27]

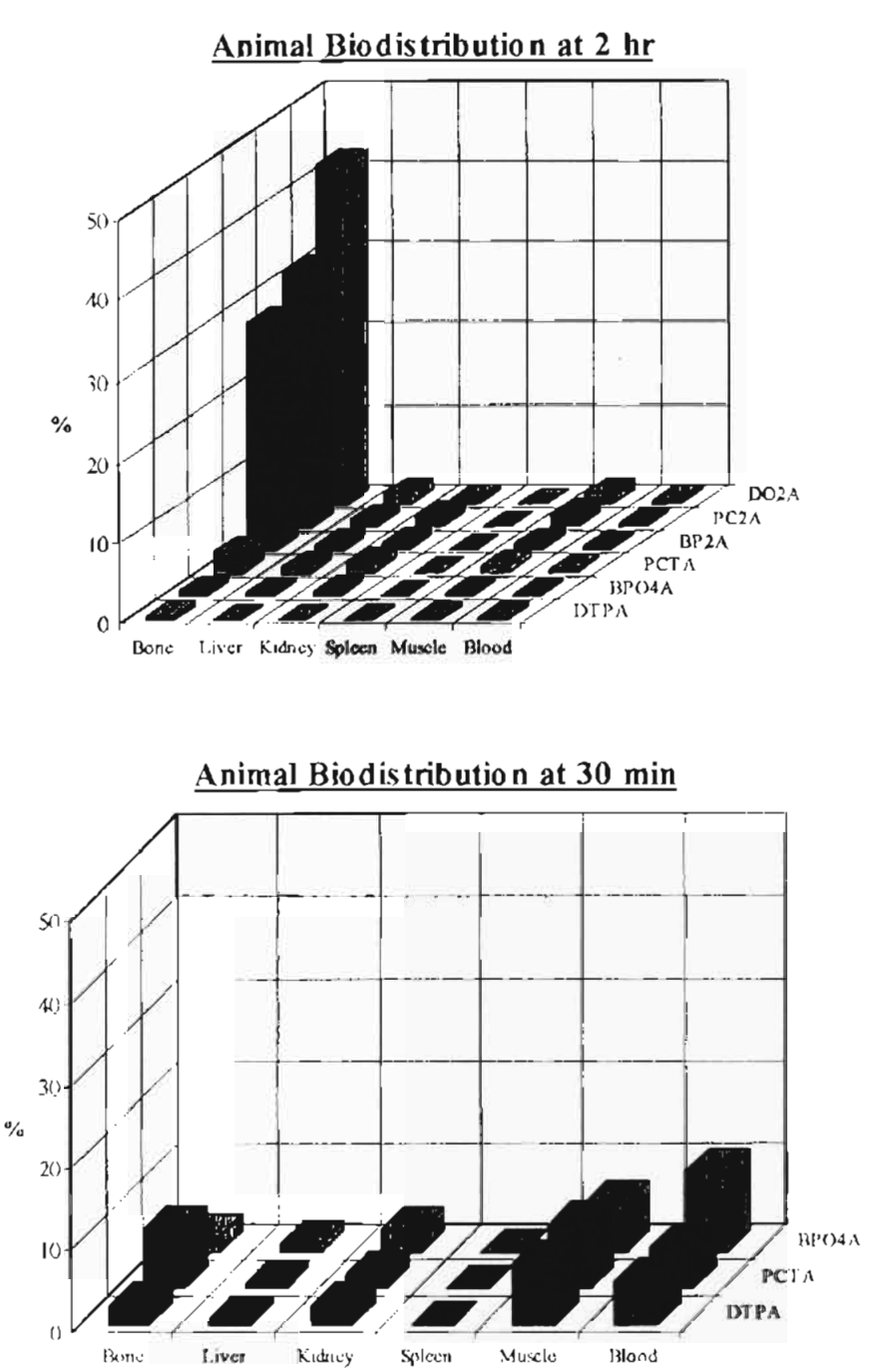

Figure 8. Top: Biodistribution of radioactive (^{153}Sm or ^{159}Gd) metal complexes in rat tissue at 2 h. Data from the complexes studied in this study [Gd(PC2A)$^{+}$, Gd(BP2A)$^{+}$, Gd(PCTA)^{0}, and Gd(BPO4A)$^{-}$] are presented with a cationic analogue, Gd(DO2A)$^{+}$, and the industry standard, Gd(DTPA)$^{2-}$. Note that a large amount of radioactivity was detected for cationic complexes even after 2 h. Bottom: Biodistribution of radioactive (^{153}Sm or ^{159}Gd) metal complexes in rat tissue at 30 min. Two noncationic complexes, Gd(BPO4A)$^{-}$ and Gd(PCTA)^{0}, are presented with Gd(DTPA)$^{-}$.

To our knowledge, these are the first examples of cationic lanthanide metal ion ligand complexes displaying bone specificity.

To clarify if indeed the cationic complexes were being taken up by bone and to rule out trans-chelation of the metal ion with the bone surface, we also performed *in vitro* absorption experiments of these Tb complexes on hydroxyapatite, $Ca_{10}(PO_4)_6(OH)_2$, as a model of bone surface.[28] In these *in vitro* absorption studies, we found that while the cationic Tb(PC2A)$^{+}$ complex absorbed very strongly on the hydroxyapatite surface as an intact complex (as evidenced by strong fluorescence of the dried column material), the neutral, Tb(PCTA)^{0}, and anionic, Tb(BPO4A)$^{-}$, complexes did not. In separate experiments, pieces of bone removed from animals after infusion of Tb(PC2A)$^{+}$ or Tb(BP2A)$^{+}$ examined under fluorescence microscope showed quite clearly that the cationic complexes were bound to the bone surface as intact complexes.[29] The mechanism of the bone uptake is still not clear but we think these

(27) (a) Simon, J.; Wilson, D. A.; Volkert, W. A.; Troutner, D. E.; Goeckeler, W. F. U.S. Patent 5,066,478. (b) Simon, J.; Wilson, D. A.; Volkert, W. A.; Garlich J. R.; Troutner, D. E. U.S. Patent 5,064,633. (c) Simon, J.; Wilson, D. A.; Volkert, W. A.; Garlich J. R.; Troutner, D. E. U.S. Patent 5,059,412. (d) Garlich J. R.; Simon, J.; Masterson, T. T. U.S. Patent 4,937,333. (e) Simon, J.; Wilson, D. A.; Volkert, W. A.; Troutner, D. E.; Goeckeler, W. F. U.S. Patent 4,898,724. (f) Simon, J.; Garlich, J. R.; Wilson, D. A.; McMillan, K. U.S. Patent 4,882,142.

(28) Kelley, W. N.; Harris, E. D., Jr.; Ruddy, S.; Sledge, C. B. *Textbook of Rheumatology*; 2nd ed.; W. B. Saunders Co.: Philadelphia, PA, 1985.

(29) Kiefer, G. E. Data to be reported elsewhere.

complexes may mimic biological cations (Ca^{2+}, K^+, Na^+, etc.) interacting with the anionic bone surface.

In the animal biodistribution studies we adopted, as a standard protocol, a dose level of 2×10^{-4} mmol/kg which is designed to reflect a broad range of nuclear medicine applications. The biodistribution results were intended to serve as a guide for assessing *in vivo* complex stability and tissue specificity. Since typical dose levels (i.e., 0.1 mmol/kg) of MRI contrast agents are several orders of magnitude greater than the nuclear medicine doses, we might expect some variations in biodistribution at higher chelate concentrations.

Acknowledgment. We thank Drs. R. A. Caldwell and A. M. Helms for assistance with luminescence lifetime measurements. This work was supported by grants from the Robert A. Welch Foundation (AT-584) and Dow Chemical Company (for portions of the research performed at UTD).

IC940854I